Photon-Statistics Excitation Spectroscopy of a Single Two Level System

Max Strauß,[1] Marlon Placke,[1] Sören Kreinberg,[1] Christian Schneider,[2]
Martin Kamp,[2] Sven Höfling,[2,3] Janik Wolters,[1,4] and Stephan Reitzenstein[1]

[1] *Institut für Festkörperphysik, Quantum Devices Group, Technische Universität Berlin, Hardenbergstraße 36, EW 5-3, 10623 Berlin, Germany*
[2] *Technische Physik, Physikalisches Institut, Wilhelm Conrad Röntgen Center for Complex Material Systems, Universität Würzburg, 97074 Würzburg, Germany*
[3] *SUPA, School of Physics and Astronomy, University of St. Andrews, St. Andrews KY16 9SS, United Kingdom*
[4] *Present address: Department of Physics, University of Basel, Klingelbergstraße 82, CH-4056 Basel, Switzerland*

We investigate the influence of the photon statistics on the excitation dynamics of a single two level system. A single semiconductor quantum dot represents the two level system and is resonantly excited either with coherent laser light, or excited with chaotic light, with photon statistics corresponding to that of thermal radiation. Experimentally, we observe a reduced absorption cross-section under chaotic excitation in the steady-state. In the transient regime, the Rabi oscillations observable under coherent excitation disappear under chaotic excitation. Likewise, in the emission spectrum the well-known Mollow triplet, which we observe under coherent drive, disappears under chaotic excitation. Our observations are fully consistent with theoretical predictions based on the semi-classical Bloch equation approach.

The fermionic two level system (TLS) is the prototype of a quantum system. As a realization of the quantum bit it finds a plethora of applications in quantum information processing [1–3]. Hence it is not surprising that two level systems under coherent excitation, e.g. under excitation with laser light or microwaves, are vastly studied and constitute a principal topic in any textbook on quantum physics. Today, the interaction of individual TLSs with coherent radiation or even single photons is routinely studied in many experiments with single atoms and ions in the gas phase, defect centers in wide bandgap materials or semiconductor quantum dots [4–6]. These experiments form the basis of many exciting applications in quantum technology. Interestingly, while the case of non-classical excitation statistics has been studied in various works[7,8], to the best of our knowledge, until now the influence of thermal excitation statistics on single TLSs has not been experimentally explored, neither in atomic nor in solid state systems. The underlying physics of this open question is of great interest from a fundamental point of view and is also motivated by the fact that coherent excitation conditions are rather artificial as virtually all radiation occurring in nature, e.g. black-body radiation or bremsstrahlung, is of chaotic nature.

In this work we set out to experimentally investigate the resonant excitation of single semiconductor quantum dots in the so far unexplored regime of resonant driving with chaotic light. In our comprehensive studies we compare fluorescence intensity, emission spectra and dynamics of a two level system represented by a semiconductor quantum dot (QD) under excitation with coherent and chaotic light. In the steady-state, we find a reduced absorption cross-section under chaotic excitation. In addition, in the emission spectrum the well-known Mollow triplet present under coherent drive of the TLS disappears under chaotic excitation, and likewise no signatures of Rabi oscillations are observed in the time domain. At the same time, the non-classical character of the photon emission of the TLS is preserved under chaotic excitation, as shown in second order auto-correlation measurements. All of these experimental findings are in excellent agreement with a quantum mechanical description of the experimental condition.

Coherent light exhibits a Poissonian photon number distribution, where the probability $p_{\mathrm{pd}}(n)$ to observe a certain photon number n is given by

$$p_{\mathrm{pd}}(n) = \frac{\langle\hat{n}\rangle^n \exp(-\langle\hat{n}\rangle)}{n!}, \tag{1}$$

where the mean photon number is $\langle\hat{n}\rangle = \langle\hat{a}^\dagger\hat{a}\rangle$, with the conventional creation (annihilation) operator $\hat{a}^\dagger$ ($\hat{a}$). The standard deviation of the photon number is given by $\Delta n = \sqrt{\langle\hat{n}\rangle}$ and for large $\langle\hat{n}\rangle$ the intensity fluctuations become negligible. Assuming stationarity, the second order auto-correlation function

$$g^{(2)}(\tau) = \frac{\langle : \hat{n}(0)\hat{n}(\tau) : \rangle}{\langle\hat{n}(0)\rangle^2}, \tag{2}$$

with : ... : indicating normal ordering, is constant $g^{(2)}(\tau) = 1$. Conventional laser radiation well above the laser threshold is a very accurate realization of such coherent light.

In contrast, chaotic light follows the Bose-Einstein statistics and the probability $p_{\mathrm{ch}}(n)$ to observe a certain photon number n is given by

$$p_{\mathrm{ch}}(n) = \frac{\langle\hat{n}\rangle^n}{(1+\langle\hat{n}\rangle)^{n+1}}. \tag{3}$$

The fluctuations of the photon number are given by $\Delta n = \sqrt{\langle\hat{n}\rangle + \langle\hat{n}\rangle^2}$. For large $\langle\hat{n}\rangle$ the fluctuations of the photon number are on the order of the average photon number $\langle\hat{n}\rangle$. Assuming stationarity, the Fourier transform of the

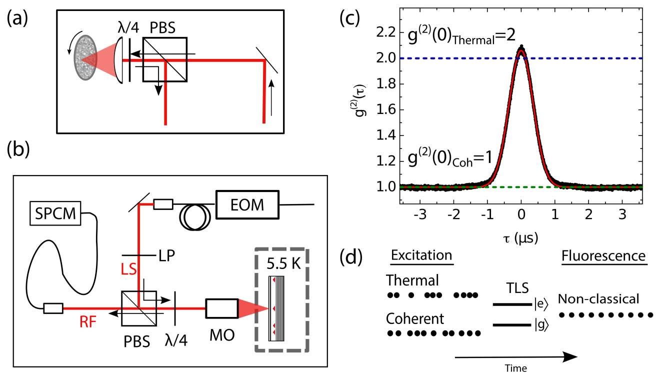

FIG. 1. (Color online) (a) Sketch of the implemented Martienssen lamp. (b) Sketch of experimental setup: Polarization filtering used to distinguish resonant fluorescence (RF) from light source (LS). Akronyms used in sketch: EOM *electro optical modulator*, LP *linear polariser*, MO *microscope objective* PBS *polarising beam splitter* SPCM *single photon counting module* (c) Measured $g^{(2)}(\tau)$-function of the chaotic light source. The red, solid line is a fit of $f(\tau) = 1 + A\exp(-\pi(\frac{\tau}{\tau_{\rm corr}})^2)$ to the data giving a correlation time of 0.9 μs. (d) Simplified picture of experiment illustrating different photon statistics involved in the experiment.

spectrum $g^{(1)}(\tau) = \langle \hat{a}^\dagger(0)\hat{a}(\tau)\rangle/\langle\hat{n}\rangle$ of a chaotic light field determines its second order auto-correlation function:

$$g^{(2)}(\tau) = 1 + |g^{(1)}(\tau)|^2. \tag{4}$$

Obviously $g^{(2)}(0) = 2$, i.e. chaotic light shows photon bunching leading to considerable effects in non-linear spectroscopy, e.g. an enhanced two-photon absorption probability [9–11]. Ideal black-body radiation, or emission from an infinite number of independent emitters are natural sources of chaotic light [12]. However, as these sources have limited spectral brightness and étendue, their use in nonlinear spectroscopy is very restricted. To circumvent these limitations, we implement a chaotic light source with a Gaussian spectrum, also known as Martienssen lamp [13–15], by reflecting a focused laser beam on a circular diffuser (1500 Grit) moving with a constant velocity of $v \approx 10\,$m/s at a radius of 10 mm (see Fig. 1 (a)). The diffuse reflection on the multitude of moving scatterers introduces Doppler broadening of the spectrum and chaotic intensity fluctuations. Fig. 1 (c) shows the measured second-order autocorrelation function of the used source, exhibiting a second-order correlation time of $\tau^{(2)}_{\rm corr} = (901.8 \pm 0.9)\,$ns according to a Gaussian fit (red trace) of the correlation function. The correlation time of the thermal field can be altered by adjusting the angular frequency of the diffuser. Furthermore, the $g^{(2)}(0)$ value of 2.05 shows that the source produces light with almost perfect thermal statistics at an emission linewidth of 1.1 MHz, where the slight deviations can be attributed to mechanical instabilities of the setup leading to an increased bunching.

As TLS we use single self assembled InGaAs quantum dots emitting between 918-930 nm grown by molecular beam epitaxy (MBE) embedded in a planar low-Q distributed Bragg reflector (DBR) cavity consisting of 24 lower and 5 upper mirror pairs. The presence of naturally occurring, micron sized photonic defects on the sample enhances the brightness of the photon flux [16]. The sample is mounted inside a helium flow cryostat and kept at a constant temperature of 5.5 K. For experiments with coherent excitation light, we use a commercial continuous wave (cw) external cavity diode laser which is focused on to the sample using a microscope objective (NA 0.65). A low power, non-resonant He-Ne laser ($<$ 0.1 nW, 637 nm) is used fill adjacent charge traps thus effectively gating the quantum dot fluorescence [17]. Directly reflected light is suppressed with a ratio exceeding 10^6 by a combination of polarization and spatial filtering prior to detection, while photons scattered by the QD are detected by a single photon counting module (SPCM) (cf. Fig. 1 (b)).

For simulating the coherent excitation experiments, we follow the semi-classical Bloch equation approach [18]. This is well justified, as for moderate laser powers of a few hundred nW, the average photon number of the excitation $\langle\hat{n}\rangle$ during the lifetime of the emitter are large and the relative photon number fluctuations $\delta n = \Delta n/\langle\hat{n}\rangle$ can be neglected. In the present case with an excitation power on the order of 100nW and a radiative lifetime of about 1 ns we estimate $\langle\hat{n}\rangle$=460 and $\delta n = 4.7 * 10^{-2}$. Taking this estimate into account, we consider the Rabi frequency $\Omega \sim \sqrt{\langle\hat{n}\rangle}$ fixed, i.e. not subject to quantum fluctuations. In this regime the resonance fluorescence intensity is directly proportional to the average exciton population $\langle\rho_{\rm X}(t)\rangle_{\rm pd}$.

In the steady state one finds

$$\langle\rho_{\rm X}\rangle_{\rm pd} = \frac{1}{2}\frac{\Omega^2 T_1/T_2}{\Delta\omega^2 + 1/T_2^2 + \Omega^2 T_1/T_2}, \tag{5}$$

with $\Delta\omega$ being the laser detuning with respect to exact resonance, T_1 the exciton lifetime in the QD and T_2 the coherence time of the exciton [19].

For chaotic light with a correlation time much longer than the coherence time of the TLS ($T_2 \leq 1\,$ns), the TLS's response can be calculated by averaging the excited state population $\langle\rho_{\rm X}(t)\rangle_{\rm pd}$ over the photon number distribution given in Eq. 3:

$$\begin{aligned}\langle\rho_{\rm X}\rangle_{\rm ch} &= \sum_n p_{\rm ch}(n)\langle\rho_{\rm X}(n)\rangle_{\rm pd}\\ &\approx \int_0^\infty {\rm d}\Omega^2\,\frac{\langle\rho_{\rm X}\rangle_{\rm pd}}{\bar{\Omega}^2}\exp\left(-\Omega^2/\bar{\Omega}^2\right), \end{aligned} \tag{6}$$

where $\bar{\Omega}$ is the Rabi frequency corresponding to a coherent light field with the same average intensity and the last line holds for large average photon numbers $\langle\hat{n}\rangle$ [12]. The integral in Eq. 6 can be solved analytically [20] and it turns out that excitation of a TLS with chaotic light is always less effective than excitation with coherent light. This can be intuitively understood, as only one photon is absorbed to generate an exciton and the remaining

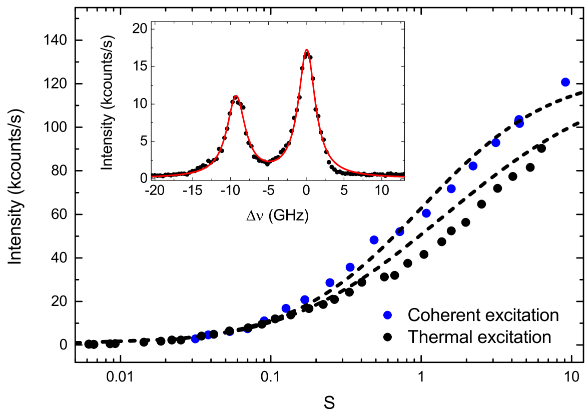

FIG. 2. (Color online) Blue (Black) dots: Saturation behaviour of TLS under coherent (chaotic) excitation. The dashed lines represent simulations of the respective experimental conditions. The inset shows the laser scan across resonance at an intensity of S=0.1. Two excitonic transitions are visible with a finestructure splitting of 9.1 GHz (37.6 μeV). The absolute energy at $\Delta\nu = 0$ is 1.34678 eV(920.6 nm). The excitation power is rescaled in units of the dimensionless saturation parameter $S = I/I_{\rm sat} = \Omega^2 T_1 T_2$ where the saturation intensity $I_{\rm sat}$ is extracted from a fit of the coherent data to equation 5.

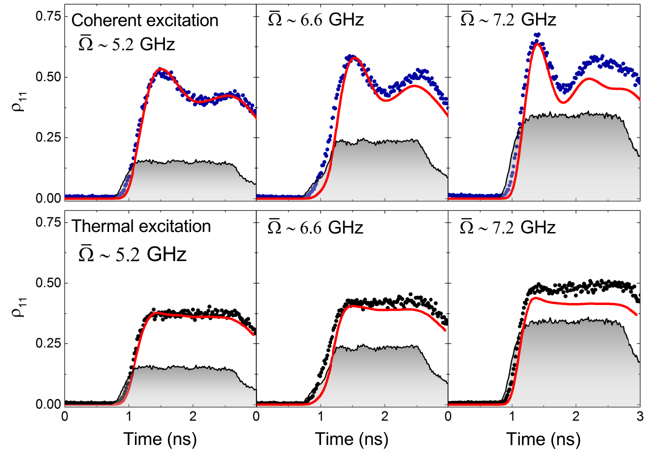

FIG. 3. (Color online) Time trace (dots) of light scattered by a single QD upon resonant excitation by 2 ns square pulses (rescaled: filled curves). Upper panel: Excitation by coherent light shows Rabi oscillations of the exciton for three different average Rabi frequencies $\bar{\Omega}$ (approximately 5.2, 6.6 and 7.2 GHz, respectively). Lower panel: Excitation by chaotic light by pulses of the same intensity creates no oscillations. The solid line represent simulations based on the optical Bloch equations as described in the main text.

bunched photons cannot be absorbed by the TLS. The theoretical prediction of Eq. 6 is in good agreement with the measurement shown in Fig. 2.

In the transient regime, the well-known Rabi oscillations are the most prominent feature of two level systems interacting with a coherent field. While quantum fluctuations of a coherent field can in principle lead to marked deviations from the classical light field, e.g. the collapse and subsequent revival of Rabi oscillations [21,22], their influence on our experiments is negligible as discussed above. For chaotic light, this regime has been studied theoretically and it has been predicted that Rabi oscillations should be suppressed by the fluctuations present in chaotic fields [23]. To experimentally verify these predictions, we use an electro-optical modulator (EOM) to temporally shape the emission of the cw light source into square pulses with a length of 2 ns and a repetition rate of 10 MHz. The arrival times of photons scattered by the QD are recorded and histogrammed over an integration time of a few minutes. The measurements under coherent resonant excitation of the TLS are depicted in the upper panel in Fig. 3. They show clear Rabi oscillations being damped by radiative and pure dephasing present in the solid state system [24,25]. This result is in excellent agreement with the numerical solutions of the semi-classical Bloch equations, where $T_2 = (325 \pm 5)$ ps and $T_1 = (641 \pm 62)$ ps were determined from independent linewidth and $g^{(2)}(\tau)$ measurements, respectively. In stark contrast, the time resolved fluorescence signal upon chaotic excitation bears no signatures of coherence generated in the TLS. This is a direct consequence of the pronounced intensity fluctuations of the chaotic field.

Besides Rabi oscillations, the iconic Mollow triplet is a further hallmark of resonance fluorescence using coherent excitation. It consists of one central peak (at frequency ν_0) and two symmetrically shifted satellite peaks (at $\nu_0 \pm \Omega$). It is a consequence of the interaction of a two level system with an intense coherent light field and can be handily interpreted in the framework of dressed states as was first proposed by Cohen-Tannoudji et al. [26]. However, this picture only holds in the the case of $\langle \hat{n} \rangle \gg \langle \Delta\hat{n} \rangle \gg 1$, which is true for a coherent state but not for chaotic light where $\langle \hat{n} \rangle = \langle \Delta\hat{n} \rangle$. Thus, for the chaotic case, it has been predicted that the two satellite peaks should disappear [20,27].

To experimentally observe the satellite peaks which are purely part of the incoherently scattered fraction of the total fluorescence at high excitation power we use a scanning Fabry-Perot resonator with a free spectra range of 26.4 GHz (109.4 μeV) and a resolution of 175.4 MHz (725.4 neV). Plotted in Fig. 4 (a) is the right wing of the Mollow triplet (T-line) under strict resonant excitation for three different average Rabi frequencies. The satellite peak is clearly visible under coherent excitation. The experimental data is in good agreement with the predicted power spectrum including pure dephasing[28]. Excitation induced dephasing which leads to a broadening of the Mollow sidepeaks at high excitation power[29], is not included in the theory and therefore likely to cause the deviations between theory and experiment at higher Rabi

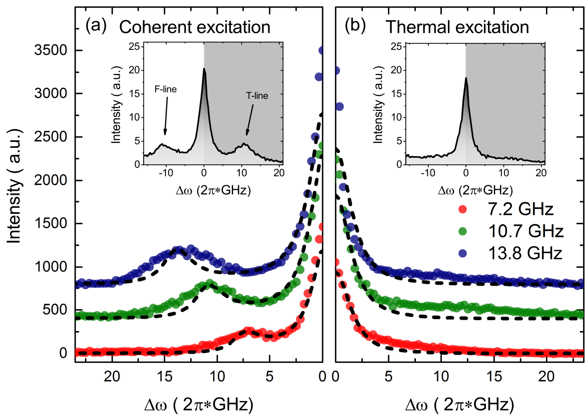

FIG. 4. (Color online) Emission spectrum of the strongly driven QD for three different average Rabi frequencies. The panel (a) on the left displays the results obtained for coherent excitation. The T-line of the Mollow triplett is clearly visible. Inset: Complete emission spectrum highlighting displayed part of Mollow triplet. For chaotic excitation, shown in panel (b), no sidepeaks are discernible. The dashed lines represent simulations corresponding to the experimental conditions.

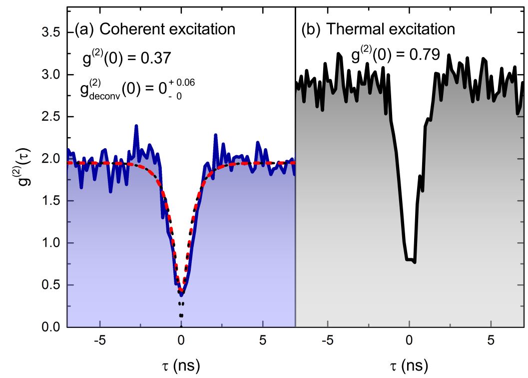

FIG. 5. (Color online) $g^{(2)}(\tau)$-measurement of the emitted radiation. The excitonic transition is driven at a Rabi frequency of $\Omega \approx 1.7\,\mathrm{GHz}$ (0.6 S). (a) Measurement using the laser as light source (solid line). The dashed line shows a convolution of the solution for a two-level system with the detector response and provides very good agreement with the experimental data. (b) Measurement using the Martienssen lamp as light source. In both measurements pronounced antibunching is visible at $\tau = 0$.

frequencies.

In contrast, under chaotic excitation (Fig. 4 (b)) the Mollow triplet cannot be observed under otherwise identical excitation conditions. This is again a direct consequence of the large intensity fluctuations present in the chaotic light field and can be quantitatively explained by averaging the power dependent spectra over the photon number distribution given in Eq. (3). In the experiments, this is achieved by integrating over times at least 5 orders of magnitude longer than the correlation time of our chaotic light source. This ensures that a thermal photon number distribution is sampled over the course of each integration interval meaning also that we average over the entire range of Rabi frequencies present under chaotic excitation.

While the previous experiments have shown that the interaction of a TLS with a light field differs significantly depending on the photon statistics inherent in the exciting light field, it is also very interesting to explore its influence on the emission statistics of the TLS.

For this purpose, a Hanbury-Brown and Twiss setup consisting of a fiber-based 50:50 beam splitter and two SPCMs (timing resolution 351 ps) is used to measure the second-order autocorrelation function. In Fig. 5 (a), the measured $g^{(2)}(\tau)$, normalized to the average count rate during the experiment under coherent excitation is shown. Superimposed onto the antibunching dip at $\tau = 0$, as is expected for a single TLS, pronounced bunching is observed for larger τ. This is typical for resonance fluorescence experiments on QDs and is attributed to blinking of the QD [30]. In Fig. 5 (b) the same measurement is shown for chaotic excitation. Here, the antibunching is visible with an increased bunching compared to the coherent case. Thus, as intuitively expected, the non-classical nature of the emitted radiation is preserved irrespective of the photon statistics of the exciting light field. While for an ideal TLS a quasi-stationary value of 2 is expected for $T_1 < \tau < \tau_{\mathrm{corr}}$ under chaotic excitation[31], we observe an increased bunching ($g^{(2)}(\tau) = 3$). This is probably caused by the blinking behaviour of the QD already visible under coherent excitation. Interestingly, the different bunching behaviour under thermal and coherent excitation indicates that the photon statistics of the excitation influences the carrier distribution and occupation dynamics of QDs which could be a topic of further investigations beyond the scope of the present work. In this regard, it is also noteworthy that without careful renormalisation of the autocorrelation data no direct difference between the two types of excitation would be observable.

In conclusion, our experiments show that the response of a quantum mechanical two level system is very sensitive to the photon statistics of the exciting light field. While differences are already visible in the saturation behavior of the TLS, the more striking differences occur in the transient regime, where Rabi oscillations are suppressed under chaotic excitation. Furthermore, the emission spectrum under strong excitation depends dramatically on the higher order correlation functions of the exciting light field. Thus, the iconic Mollow triplet disappears under chaotic excitation. With its nonlinear nature, the fermionic TLS is an ideal probe for the fluctuations present in the light field. Future experiments will be directed towards exploring the regime of short correlation times in the excitation field, being on the order of or even shorter than the coherence time of the TLS. Also, extending photon-statistics excitation spectroscopy to non-classical light sources will be highly interesting.

We thank M. Aßmann and A. Carmele for stimulating discussions. The research leading to these results has received funding from from the European Research Council under the European Union's Seventh Framework ERC Grant Agreement No. 615613 and from the German Research Foundation via the project RE2974/5-1.

---

[1] M. H. Devoret and R. J. Schoelkopf, Science **339**, 1169 (2013).
[2] J. Wrachtrup and F. Jelezko, J. Phys. Condens. Matter **18**, S807 (2006).
[3] M. Nielsen and I. Chuang, Quantum Computation and Quantum Information (Cambridge University Press, Camebridge, 2010).
[4] D. Leibfried, R. Blatt, C. Monroe, and D. Wineland, Rev. Mod. Phys. **75**, 281 (2003).
[5] H. M. Meyer, R. Stockill, M. Steiner, C. Le Gall, C. Matthiesen, E. Clarke, A. Ludwig, J. Reichel, M. Atatüre, and M. Köhl, Phys. Rev. Lett. **114**, 123001 (2015).
[6] J. Wolters, M. Strauß, R. S. Schoenfeld, and O. Benson, Phys. Rev. A **88**, 020101 (2013).
[7] N. P. Georgiades, E. S. Polzik, K. Edamatsu, H. J. Kimble, and A. S. Parkins, Phys. Rev. Lett. **75**, 3426 (1995).
[8] K. W. Murch, S. J. Weber, K. M. Beck, E. Ginossar, and I. Siddiqi, Nature **499**, 62 (2013).
[9] A. Carmele, A. Knorr, and M. Richter, Phys. Rev. B **79**, 035316 (2009).
[10] T. Kazimierczuk, J. Schmutzler, M. Aßmann, C. Schneider, M. Kamp, S. Höfling, and M. Bayer, Phys. Rev. Lett. **115**, 027401 (2015).
[11] F. Boitier, A. Godard, E. Rosencher, and C. Fabre, Nat. Phys. **5**, 267 (2009).
[12] R. Loudon, The Quantum Theory of Light, 3rd ed. (Oxford University Press, Oxford, 2001).
[13] W. Martienssen and E. Spiller, Am. J. Phys. **32**, 919 (1964).
[14] F. T. Arecchi, Phys. Rev. Lett. **15**, 912 (1965).
[15] W. Martienssen and E. Spiller, Phys. Rev. Lett. **16**, 531 (1966).
[16] S. Maier, P. Gold, A. Forchel, N. Gregersen, J. Mørk, S. Höfling, C. Schneider, and M. Kamp, Opt. Express **22**, 8136 (2014).
[17] H. S. Nguyen, G. Sallen, C. Voisin, P. Roussignol, C. Diederichs, and G. Cassabois, Phys. Rev. Lett. **108**, 057401 (2012).
[18] L. Allen and J. Eberly, Optical resonance and two-level atoms (Dover, 1975).
[19] E. B. Flagg, a. Muller, J. W. Robertson, S. Founta, D. G. Deppe, M. Xiao, W. Ma, G. J. Salamo, and C. K. Shih, Nat. Phys. **5**, 203 (2009).
[20] A. T. Georges, P. Lambropoulos, and P. Zoller, Phys. Rev. Lett. **42**, 1609 (1979).
[21] G. Rempe, H. Walther, and N. Klein, Phys. Rev. Lett. **58**, 353 (1987).
[22] S. Mukamel and K. E. Dorfman, Phys. Rev. A **91**, 053844 (2015).
[23] P. Knight and P. Radmore, Phys. Lett. A **90**, 342 (1982).
[24] A. J. Ramsay, A. V. Gopal, E. M. Gauger, A. Nazir, B. W. Lovett, A. M. Fox, and M. S. Skolnick, Phys. Rev. Lett. **104**, 017402 (2010).
[25] A. V. Kuhlmann, J. H. Prechtel, J. Houel, A. Ludwig, D. Reuter, A. D. Wieck, and R. J. Warburton, Nat. Commun. **6**, 8204 (2015).
[26] C. Cohen-Tannoudji and S. Reynaud, J. Phys. B At. Mol. Phys. **10**, 345 (1977).
[27] P. Avan and C. Cohen-Tannoudji, J. Phys. B **155**, 117 (1977).
[28] C. Matthiesen, A. N. Vamivakas, and M. Atatüre, Phys. Rev. Lett. **108**, 093602 (2012).
[29] S. M. Ulrich, S. Ates, S. Reitzenstein, A. Löffler, A. Forchel, and P. Michler, Phys. Rev. Lett. **106**, 247402 (2011).
[30] A. Ulhaq, S. Weiler, S. M. Ulrich, R. Roßbach, M. Jetter, and P. Michler, Nat. Photonics **6**, 238 (2012).
[31] M. Schubert, K.-E. Süsse, and W. Vogel, Opt. Commun. **30**, 275 (1979).